View metadata, citation and similar papers at core.ac.uk

brought to you by CORE

provided by Chalmers Research

Characteristics of homogeneous multi-core fibers for SDM transmission

Downloaded from: https://research.chalmers.se, 2020-07-11 02:56 UTC

Citation for the original published paper (version of record):

Puttnam, B., Luis, R., Rademacher, G. et al (2019)
Characteristics of homogeneous multi-core fibers for SDM transmission
APL Photonics, 4(2)
http://dx.doi.org/10.1063/1.5048537

N.B. When citing this work, cite the original published paper.

research.chalmers.se offers the possibility of retrieving research publications produced at Chalmers University of Technology.
It covers all kind of research output: articles, dissertations, conference papers, reports etc. since 2004.
research.chalmers.se is administrated and maintained by Chalmers Library

(article starts on next page)

Characteristics of Homogeneous Multi-Core Fibers for SDM Transmission

Benjamin J. Puttnam[1], Ruben S. Luís[1], Georg Rademacher[1], Arni Alfredsson[2]
Werner Klaus[1], Jun Sakaguchi[1], Yoshinari Awaji[1], Erik Agrell[2] and Naoya Wada[1]

[1]*Photonic Network System Laboratory, National Institute of Information and Communications Technology (NICT), 4-2-1 Nukui-Kitamachi, Koganei, Tokyo 184-8759, Japan.*
[2]*Department of Electrical Engineering, Chalmers University of Technology, SE-412 96 Gothenburg, Sweden.*

We describe optical data transmission systems using homogeneous, single-mode, multi-core fibers (MCFs). We first briefly discuss space-division multiplexing fibers, observing that no individual SDM fiber offers overwhelming advantages over bundles of single-mode fiber (SMF) across all transmission regimes. We note that for early adoption of SDM fibers, uncoupled or weakly coupled fibers which are compatible with existing SDM infrastructure have a practical advantage. Yet, to be more attractive than parallel SMF, it is also necessary to demonstrate benefits beyond improved spatial spectral efficiency. It is hoped that the lower spread of propagation delays (skew) between spatial channels in some fibers can be exploited for improved performance and greater efficiency from hardware sharing and joint processing. However, whether these benefits can be practically harnessed and outweigh impairments or effort to mitigate crosstalk between spatial channels is not yet clear. Hence, focusssing on homogeneous MCFs, we first describe measurements and simulations on the impact of inter-core crosstalk in such fibers before reporting experimental investigation into the spatial channel skew variation with a series of experimental results including a comparison with SMF in varying environmental conditions. Finally, we present some system and transmission experiments using parallel recirculating loops that enable demonstration of both multi-dimensional modulation and joint digital processing techniques across three MCF cores. Both techniques lead to increased transmission reach but highlight the need for further experimental analysis to properly characterize the potential benefits of correlated propagation delays in such fibers.

1. INTRODUCTION

Optical transmission systems and networks underpin the digital economy and form a key part of the worldwide communications infrastructure. However, ongoing provision of new services and larger data volumes required to meet the needs of businesses, academia, governments and citizens provide new challenges to optical communication infrastructure with operators also facing commercial pressure to offer them at ever lower cost per bit. In the research community this has led to the exploration of advanced optical fibers to replace the standard single mode fiber (SMF) which has dominated commercial fiber systems for decades. Broadly described as space-division-multiplexing (SDM) [1] , this research field refers to fibers that allow data transmission in parallel strands of SMF, a combination of multiple cores within a single cladding or multiple modes in a single core [2]. In each case, the aim is typically to both increase the achievable data throughput and also to encourage energy and resource savings, hardware integration and joint signal-processing. Transmission demonstrations over single-mode(SM)-multi-core fibers (MCFs) have been demonstrated with up to 32 cores [3] and few-mode or multi-mode fibers (both subsequently referred to as FMFs) with up to 45 modes [4]. Combining few-mode cores in multi-core fibers has enabled single optical fibers with over 100 spatial channels [5], [6] and total transmission throughputs of over 10 Pb/s [7] albeit with significantly enlarged cladding diameters.

SM-MCFs potentially offer the simplest migration path for adoption of SDM fibers as they allow a phased upgrade path from conventional fiber bundles where the fiber, SDM amplifiers or shared transmitter and receiver hardware may be introduced in stages whilst being compatible with existing SMF systems. SM-MCFs fibers have been shown to support wide

band, high spectral efficient (SE) modulation without the need for high-order multiple-input/multiple-output (MIMO) based receivers [3], [8], [9]. Within weakly coupled MCFs, there is a further distinction between homogeneous core MCFs, where near identical core properties are targeted, and heterogeneous core structures where neighboring cores are designed to have variations in refractive index in order to reduce inter-core coupling. The reduced coupling typically allows higher core densities in a given core diameter, with up to 32 cores realized in a transmission grade heterogeneous MCF [3] compared to 22 for homogeneous fibers [8] with similar cladding diameter. A heterogeneous fiber was demonstrated in combination with an MCF amplifier for transmission of wavelength-division multiplexed (WDM) 16-quadrature-amplitude modulation (QAM) signals over 1600km [10]. However, the majority of transmission demonstrations to date have used homogeneous MCF including the record SM-MCF capacity [8] and the highest throughput-distance product of any optical fiber transmission [11]. Homogeneous SM-MCFs have also been extensively used in long-haul transmission [12], access [13], data-centre [14] and networking demonstrations [15]. Furthermore, the relative uniformity of the homogeneous cores supports spatial super channels (SSCs) for shared transmitter hardware, digital signal processing (DSP) resources and simplified switching [16]. In this paper, we focus on homogeneous MCFs. We first make a comparison with alternative SDM fibers, including parallel SMFs. We then describe a series of measurements investigating the limitations or benefits of their characteristic features, including inter-core crosstalk and skew. Finally, we describe system experiments demonstrating new multi-core modulation formats [17] and joint DSP [18] that can exploit low spatial channels skew and provide additional benefits that may not be gained by other forms of SDM.

2. WHY CHOOSE HOMOGENEOUS MULTI-CORE-FIBERS

A number of SDM fibers, which fall into several broad categories, have been proposed. Each fiber type has different characteristics that provide specific advantages in some transmission contexts, but no fiber type SDM fiber appears preferable to parallel SMF or ribbon fiber in all optical transmission and network scenarios. For example, coupled core MCFs (CC-MCFs) have shown to have an advantage over SMF in terms of non-linear tolerance that translates to longer transmission distances [19], in addition to benefits from joint processing and amplification [20], [21], so may thus be the best choice for long distance point-to-point links. However, FMFs or FM-MCFs offer much higher number of spatial channels in a given cladding diameter and therefore likely to be suitable for short range, high capacity links.

The primary characteristics of SDM fibers that determine their transmission performance are the level of signal mixing between spatial channels and the spread of propagation time (skew) between spatial channels. The level of mixing gives rise to two sub-groups of SDM fibers. The first group consists of coupled-core MCFs, few-mode fibers or few-mode MCFs where signals in different spatial channels are mixed during transmission. The second group, where the mixing is more commonly referred to as crosstalk (XT), is the weakly coupled SM-MCFs but also included SMF bundles if amplification, hardware-sharing or processing occurs across spatial channels.

The spatial channel skew is expected to impact the feasibility of performing joint processing and modulation across SSCs that may provide some of the benefits of SDM and is typically lowest for coupled fibers, at least between the mixed spatial sub-channels (mode group or FM-MCF core). However, the requirement for MIMO processing resulting from this mixing also prevents add/drop and routing of spatial sub-channels before reception that is potentially a key advantage of weakly-coupled fibers as the transmission medium in metro to national size networks. Of the weakly coupled fibers, heterogeneous core designs inherently introduce skew between cores and experimental measurements have shown that significantly larger skew variations observed in independent SMFs than in homogeneous cores in sharing the same cladding, making homogeneous SM-MCFs advantageous in terms of skew [22].

A further advantage of SM-MCFs in the near term is the easier migration path from existing SMF based networks. The compatibility of single mode cores allows SDM amplifiers or transceiver integration to happen before fiber installation, perhaps making such fibers more attractive to operators. However, even in this model, for migration from bundled SMF to SM-MCFs to make sense, it is still necessary to demonstrate a clear advantage of MCF transmission arising from the relatively low skew as well as to properly evaluate the impact that inter-core crosstalk can have on transmission. Hence, we devote the following sections to analysis of inter-core crosstalk, skew and experimental investigation of multi-dimensional modulation formats and joint-SDM processing.

3. INTER-CORE CROSSTALK (IC-XT) IN WEAKLY COUPLED FIBERS

Aside from bundled SMF, one challenge for adoption of SDM fibers concerns the mixing of signals in different spatial channels. For strongly coupled fibers, such as few-mode or coupled core fibers, this mixing can be a feature and it is assumed that all coupled spatial sub-channels are received together and a MIMO equalizer is used to separate them. MIMO processing has also been used to undo IC-XT in weakly coupled-fibers [23], but it is typically treated as an additional noise in MCFs. IC-XT differs from localized crosstalk in optical components in the sense that it has a stochastic behavior, varying randomly over time and wavelength within a wide dynamic range, depending strongly on the core-pitch, inter-core temporal skew, chromatic dispersion variation and signal modulation format [24]–[27]. An example of spectral and temporal variation of IC-XT is shown in Fig. 1(a) which shows the crosstalk generated by a 24.5 GHz bandwidth PDM-16QAM signal on a single core of a 7-core fibre. The measurements were made with a high resolution spectrum analyzer and show a single swept measurement as well as the maximum and minimum of each spectral component measured over a 1 hour period. The single sweep shows over 7dB variation in crosstalk between spectral components of the 24.5 GHz signal and almost 9dB between the extreme measurements in the 1 hour period. This spectral variation is the origin of the sensitivity of the XT power variance on modulation format as explained in detail in [28]. As measured in [25], crosstalk from a CW signal in a neighboring core, can vary randomly over time by 10s of decibels with a behavior depending mainly on the skew between cores and the symbol rate (spectral occupation) of the signal as well as the kind of modulation. Signals with modulation formats supported by a strong carrier, such as OOK or 4 PAM, produce crosstalk with dynamic fluctuations and a temporal profile similar to that shown in Fig. 1(b) for a CW signal. This has implications for potential adoption of homogeneous MCFs for application using formats with strong carriers as large performance margins may be required to ensure quality of service.

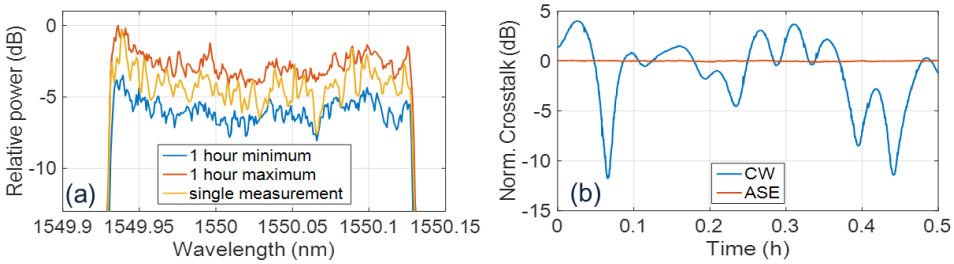

Fig.1 (a) 1 hour maximum, instantaneous and 1 hour minimum XT measurements over bandwidth of 25 GBaud signal using set-up from **[29]** and (b) crosstalk power variations in a single core from ASE and continuous wave signals in neighboring cores of homogeneous MCF

This spectral variation is the origin of the sensitivity of the XT power variance on modulation format as explained in detail in [29]. As measured in [26], crosstalk from a CW signal in a neighboring core, can vary randomly over time by 10s of decibels with a behavior depending mainly on the skew between cores and the symbol rate (spectral occupation) of the signal as well as the kind of modulation. Signals with modulation formats supported by a strong carrier, such as OOK or 4 PAM,

produce crosstalk with dynamic fluctuations and a temporal profile similar to that shown in Fig. 1(b) for a CW signal. This has implications for potential adoption of homogeneous MCFs for application using formats with strong carriers as large performance margins may be required to ensure quality of service.

The impact of fiber geometry and core pitch on the average crosstalk is illustrated in Fig. 2(a), based on the 22-core fiber also shown as an inset. This fiber, used for over 2 Pb/s transmission [30], was designed to minimize crosstalk impact by adopting a two core pitch design with a core pitch of 42 µm between neighboring cores in the same ring and larger 49 µm pitch between each ring. This means that, in contrast to other high core-density homogeneous MCFs, each core aside from the center core is mostly affected by XT from its two nearest neighboring cores. In addition to reducing crosstalk this design also lends itself to strategies to minimize crosstalk impairment such as bi-directional transmission [31] or adoption of low order MIMO processing only for the interacting cores [23]. In the lower half of Fig. 2(a), the refractive index profile of neighbouring cores in 1 ring (42 µm core pitch) and between rings (49 µm core pitch) are shown with a common reference of the mid-point between the cores. The upper half shows the normalised field distribution for light in core 1 (left side) into core 2 on the right. In addition to the field profiles for the two core pitches including the impact of the refractive index trenches shown, a 3rd line also shows the case for a 42 µm core without any refractive index trench. The plot shows that increasing core pitch by 7 µm reduces the intensity field in a neighbouring core by around 15dB and that in the case of the 42 µm core, the refractive index trench, which is relatively small compared to other fiber designs [32], [33] reduces the field power in the neighbouring core by 10dB. We note that the MCF with lowest IC-XT reported [24] (≈64.7 dB/100km at 1550 nm) used a homogeneous core design with refractive index trench of over 0.9% lower than that of the core.

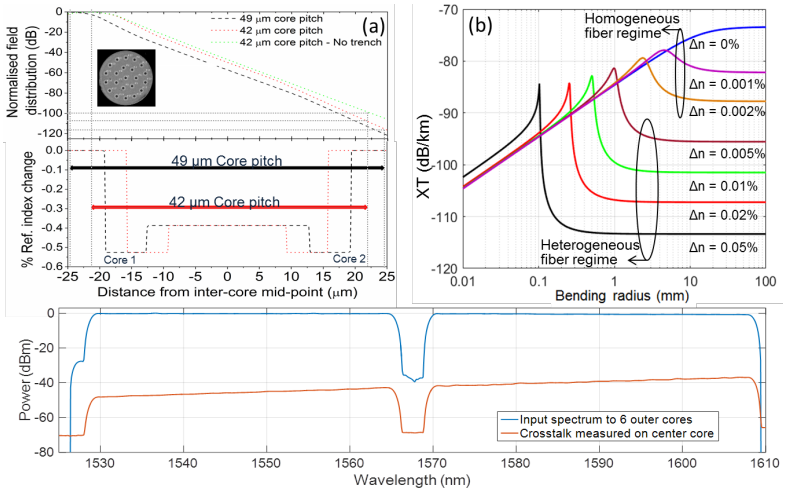

FIG.2 (a) Normalized field distribution as a function of core separation and core, cladding and trench layout for two-core pitch 22-core MCF, (b) calculated average inter-core crosstalk as a function of fiber bending radius and (c) measured wavelength dependence of inter-core crosstalk from wideband C and L band signal in 7-core MCF.

Additional fiber properties that can affect the level and impact of IC-XT in homogeneous MCFs are the bending radius and wavelength dependence of the field overlap between adjacent cores. Both the mode-coupling coefficient and propagation constant have a wavelength dependence that for both step-index and trench-assisted fibers results in a steady increase in IC-XT level with wavelength that can become a significant issue for systems utilizing transmission spectra in the long L-band. Fig. 2(c) shows the crosstalk spectrum in the center core generated by a flattened C and L-band spectrum transmitted in the 6 outer cores of a 53.7 km fiber. Both spectra were measured with a 1nm resolution show a steady increase in XT with around 11 dB higher IC-XT for channels at 1610nm compared to those at 1530 nm. The impact of the bending radius is shown in Fig. 2(b) which shows the calculated XT characteristics as a function of bending radius for various refractive index

differences, Δn, between neighboring cores assuming a 42 μm core pitch. The blue line is the case for two perfectly dentical homogeneous cores. However, n practice, some heterogeneity usually remains and although no firm definition exists, MCFs are typically considered as homogeneous for Δn values <0.002%. In the heterogeneous regime, Δn can exceed 0.3% [34] and depends on the number of heterogeneous core and fiber geometry needed to meet the target XT level. To date, few experimental investigation of the impact of bending radius have been performed, but recent measurements of an unspooled homogeneous fiber suggest that the dependence of ICXT on bending radius is not as severe as expected with little increase when XT was compared in a straightened 2 km span and the same fiber spooled with 16 cm radius [35].

4. INTER-CORE SKEW IN MULTI-CORE FIBERS

As discussed in section 2, the difference of propagation time between spatial channels and the impact this has on effective resource sharing could be an important consideration for the choice and design of SDM systems. While in practice, framing and buffering techniques may be used to mitigate their impact, large variation of propagation delays are still likely to impact the achievable symbol-rates, transmission distances, receiver design and complexity of DSP [16], [36]. This is particularly significant for transmission over many spans or in networks where paths are dynamically assigned. In the case of SMF and single mode MCFs, the spatial channel skew consists of an average skew determined by differences in the average refractive index between cores with some dynamic variation caused by variable environmental factors. For homogeneous MCFs measured thus far, the average skew is of the order of 100 ps/km [22] increasing to ns/km for heterogeneous MCFs depending on the range of Δn in the heterogeneous core design [37]. Measurements of dynamic skew at fixed temperature in laboratory conditions have been of the order of fractions of ps/km for a range of core counts and core diameters [38] [39], but similar measurements have yet to be made with heterogeneous MCFs.

Fig. 3 (a) shows the core layout of a 53.7 km 7-core fiber with the measured average skew between the center core and each outer core. The largest differential ICS of 26.8 ns, between cores 6 and 2, is approximately 500 ps/km. Both the absolute and dynamic skew of the same fiber in response to temperature variation was also measured using the set-up shown in Fig. 3 (b) and compared with independent SMFs of similar lengths as described in [22]. Light from a tunable laser at 1550nm was modulated in single polarization Mach-Zehnder modulator (MZM), driven by a pulse pattern generator (PPG) with a 2^{15}-1 pseudo random binary sequence (PRBS) to produce a 10Gb/s on-off keyed (OOK) signal. The signal was amplified by an erbium-doped fiber amplifier (EDFA). After removing ASE in a 1 nm band-pass filter, the signal was then divided in a 1 x 8 power splitter and either 7 paths directed to cores of an MCF or 2 paths to near-identical SMF links. The MCF was 53.7km and each SMF link was constructed from 2 sub-spans with those in each link having identical specifications but with slight variation in length to give a total fiber lengths of 53.2 km and 53.5 km. All the fibers were spooled with 15cm bend radius and stored vertically without external insulation.

For measurements, the fibers under test were placed in a sealed insulated chamber with facility for input/output of optical patch cords and electrical cables for temperature control and measurement. A temperature sensor was placed between fiber strands of one spool, with a programmable temperature controller (TEC) used to control heat pads held within the box. After fiber transmission, the signals from each fiber core or SMF link were received by individual photo-detectors (PDs) with integrated trans-impedance amplifiers (TIAs) designed for 10 Gbit/s OOK signals. The resulting electrical signals were then saved in a digital oscilloscope with 16GHz bandwidth and 50Gs/s sampling rate. To allow estimation of the static skew between channels, identical patch cords and electrical cables were used for all channels. In addition, the relative dynamic skew between each core and the center core could be obtained as a function of time and temperature by cross-correlating the

corresponding cores' signals. Similar to the method described in [9], μs length traces allowed averaging to remove noise and digital resampling to provide sub-picosecond accuracy verified by first measuring fluctuations in back-to-back operation.

In addition to static skew measurements, changes in the relative skew of the 6 outer MCF cores to the center core and between the 2 SMF links were then observed for periods up to 12 hours with measurements taken approximately every 3 seconds and temperatures varied between 23 °C and 45 °C. Fig. 3 (c) shows a measurement of dynamic skew fluctuations over a 12 hour period with a stable temperature of 23.5°C for both the MCF and the 2 SMF links. The 2 single mode fibers drift by over 1ns over the 12 hour period. Over the same scale the skew between different cores is difficult to distinguish and an expanded plot is shown in Fig. 3 (d). The total range of dynamic skew for 6 outer cores compared to the center core is less than 3 ps, close to 3 orders of magnitude smaller than the equivalent SMF. Fig. 3(e) shows a similar measurement for a stable temperature of 45°C. While exhibiting slightly more noise, the total largest skew variation is under 4ps in the 12 hour period.. The dynamic skew observed in the MCF is similar to previous laboratory measurements [38]. However, the SMF links showed considerable larger dynamic skew than previously observed in similar fibers [39], with the difference attributed the additional fiber and additional thermal insulation used in previous measurements.

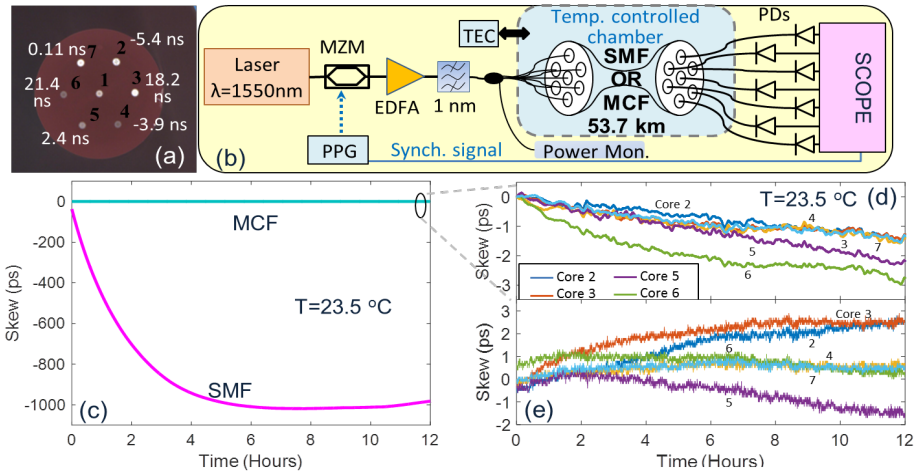

FIG.3 (a) Layout of 53.7 km 7-core fiber with the measured fixed skew of each outer core relative to the center core and (b) experimental set-up for measurement of dynamic inter-core/fiber skew fluctuations in a temperature controlled chamber (c) Comparison of skew variation between 7 cores of a 53.7 km MCF and 2 independent 53.4 km SMFs over 12 hours at stable lab temperature **[22]** and fine detail plot skew variation of individual MCF cores at (d) 23.5 °C and (e) 45 °C.

The impact of heating and cooling on the inter-core and SMF-link skew was investigated over the same temperature range. Figs. 4 (a) and (b) show the change of skew for 6 outer cores relative to the center and between the two SMF spans respectively. The upper plots show the change of skew as the temperature, shown in the lower plot, is increased from 23.5 °C to 45 °C. The heating time for the MCF was around 30 minutes longer than the SMF due to the slightly higher heat capacity of the equipment needed to support the MCF spools. For both fiber types, the temperature change induced larger relative skew between MCF cores or SMF fibers than observed at stable temperatures. In the MCF case, the skew relative to the center core ranged from -8 ps (core 7) to 62 ps (core 3). Heating of the SMF link pair changed the skew by 2.7ns, approximately 40 times larger than the MCF.

After reaching 45 °C the temperature was maintained at this value for a further 4 to 4.5 hours. During this period, the change of relative skew between MCF cores slows and after 1-2 hours the shifts are similar to those shown in Fig. 3(e). In contrast, the skew between the SMF links abruptly reversed direction and changed by a further 2.3 ns over the 4 hour period. It is possible that this behavior results from uneven heating between the 2 spans, so although the order of magnitude is similar

to the fixed temperature case, it is possible that change of skew between in the SMF case is exaggerated in this case. We also note that the impact of spooling on the heat transfer and the impact of local temperature fluctuations likely in installed fibers are not considered in these measurements.

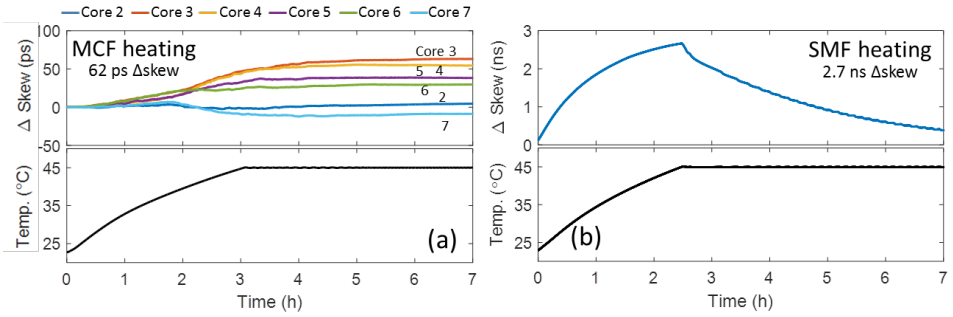

FIG. 4 (a) Skew variation between 2 independent 53km SMFs under the temperature profile shown in (c) and (b) skew variation of 6 outer cores of 53.7 km MCF compared to the center core under similar heating profile (d) over 7 hour period

Overall, it seems reasonable to conclude that spatial channel skew in homogeneous MCFs will be less than for bundled SMFs, but the importance of this remains to be seen. We note that the 300m length difference between the 2 spans is equivalent to 0.56 % of the shorter span length and although this difference may give a small increase in the measured skew variation, it cannot explain the large difference between the MCF and SMF spans observed. The static skew range of 26.8 ns measured between the most disparate cores is equivalent to 268 symbol periods at 10 GBaud transmission, much longer than the memory of typical equalizer filters of commercial DSP systems. It is of course, possible to compensate static skew with patch cords or optical delays, but it is not clear if this is feasible for links over many spans or how this will work in networks with flexible routing and path assignment. Hence, practical SSC transmission with multi-dimensional modulation and shared processing may require development of homogeneous MCFs with inherently lower skew between all core pairs or precise temperature control. Similarly, although data framing or digital buffering techniques are often proposed to overcome skew fluctuations for shared processing schemes, it will add processing complexity, increase latency and may not be practical for skew accumulated over long links, particularly when nanosecond delays can be accumulated over single spans if parallel SMFs are adopted as a first SDM implementation.

5. MULTI-CORE FIBER EXPERIMENTS

In this section we describe MCF system experiments and the challenges of performing realistic system experiments that explore benefits potentially arising from the lower spatial channel skew of MCFs described in the previous section. However, the majority of transmission demonstrations and experiments into multi-core modulation schemes [17], [40], [41] have been performed by receiving each signal core in sequence with a single modulator and receiver. Particularly for formats utilizing the soft-decision of symbols, the absence of synchronized modulation and reception makes true multi-dimensional modulation harder to implement. Furthermore, if a common laser is used, receiving signals in sequence removes correlations between the parallel spatial channels, such as correlated phase noise, that may be exploited by to gain greater efficiencies and improved performance from joint DSP. For this reason, here, we describe a series of experiments targeting more realistic MCF system experiments, combining 3 independent modulators with a common light source, joint-reception and recirculating transmission in 3 synchronized loops each using different cores of an MCF. We present experimental measurements with 2 sets of multi-dimensional modulation formats based on 16-QAM and 64-QAM constellations in each of the 3 cores before describing some experiments of joint-reception.

A. EXPERIMENTAL SET-UP

The experimental setup for multi-core transmission experiments is shown in Fig. 5. A tunable laser was set to a wavelength of 1550.12 nm and the light was then split in 1 x 3 splitter. The 3 outputs were then each directed to separate dual parallel Mach-Zehnder modulators (DP-MZM), each driven by 4 independent arbitrary waveform generators (AWG) operating at 60 GS/s with 20 GHz bandwidth to generate pre-equalized, square root-raised cosine shaped PDM-QAM signals at 20 GBaud with a 0.01 roll-off. After separate amplification, skew compensation of the combined transmitter and receiver paths was performed using patch cords and optical delays (ODs) to provide aligned path lengths within <1cm. On each path, acousto-optic modulators (AOMs) were used to gate the signals at the input to 3 independent re-circulating transmission loops with additional power control in a variable optical attenuator (VOA). Each loop contained a 3dB loop coupler to combine the input and recirculated paths. The loop output of the coupler had an EDFA followed by a 0.4nm OBPF to reduce out-of-band noise and a VOA to control launch power at the input to one core of the same 53.7 km span of a 7-core multi-core fiber, described in the preceding experiments. Each loop used one of 3 neighboring cores (1, 2 and 7 as shown in Fig 2(a)) and on each recirculation, an amplified tap of the signal from loop 3 was decorrelated in different length patch cords and used as dummy signals in each of the remaining four cores which were terminated after transmission.

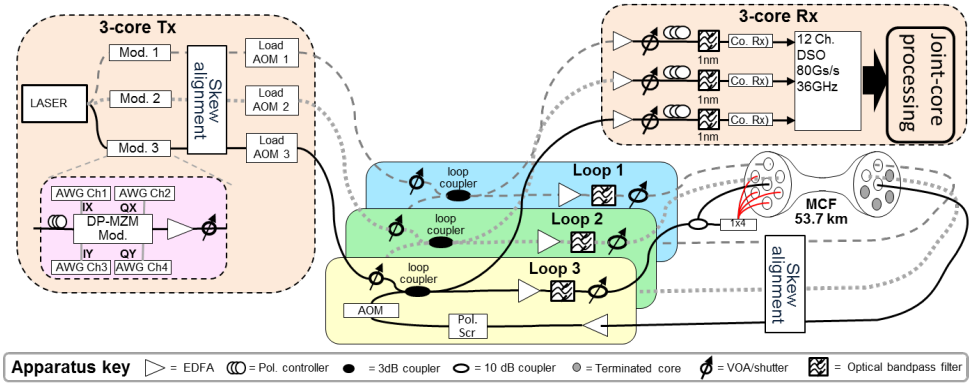

FIG. 5. Experimental set-up for exploration of multi-dimensional modulation and joint carrier-phase estimation

After fiber transmission, another amplification stage compensated for the fiber loss and another skew compensation stage was used to compensate for both the inter-core skew and path length variation in additional components in each loop to within 1cm. Finally, each loop contained a polarization scrambler (Pol. Scr.) before a second AOM was used to block the re-circulating signal during the loop-loading phase. Timing control for all 3 loops was performed in a single timing controller unit. In addition to gating the AOMs, the unit also provided a receiver gating signal and was used to trigger the Pol. Scr and optical spectrum analyzers. The recirculation time for all 3 loops was 263.9 μs and the loop output was taken from the second output of the 3dB loop coupler. Each receiver path contained an additional EDFA and VOA for power control, a polarization controller and a 1nm OBPF before a coherent receiver (CoRx). Due to component limitations, each CoRx had different electrical bandwidths of 20, 25 and 33 GHz and a 100 kHz linewidth tunable laser was split between each receiver and used as a common LO for coherent reception. The detected signals were digitized and stored for processing using a 12-channel real-time oscilloscope with a 36 GHz electrical bandwidth, operating at 80 GS/s. DSP was performed offline using MATLAB and C, similar to [8].

B. MEASUREMENTS OF 12 DIMENSIONAL MODULATION FORMATS

The set-up described above was first used to investigate a family of 12-dimensional (12-D), lattice-coded modulation schemes based on either PDM-16QAM or PDM-64QAM modulation in each of the 3 jointly received cores. The selected constellations were obtained from a set of 12-D integer lattices, which were designed to have the largest possible minimum Euclidean distance and (ii) the minimum possible nearest-neighbor multiplicity. Compared with the cubic lattice (16- or 64-QAM), the Euclidean distance is increased at the cost of reduced spectral efficiency with the number of bits per symbol being reduced by 12-k bits, where k is an integer between 4 and 12 that denotes the constellation size. Hence for the largest overhead (k = 4) formats each 3-core symbol is carries 16 information bits compared to 24 for regular PDM-16QAM (K=12) in three cores and 28 information bits instead of 36 for formats using PDM-64QAM constellations. Table 1 shows relative spectral efficiencies and squared Euclidean distances, compared with the QAM base formats.

TABLE 1 – Relative spectral efficiency (SE) and squared Euclidean distance of 12-D formats compared to regular QAM in each core

k	Squared Euclidean distance	SE - 16QAM lattice	SE - 64QAM lattice
12	1	1.00	1.00
11	2	0.96	0.97
8	3	0.83	0.89
7	4	0.79	0.86
4	6	0.67	0.78

Whilst ultimately, it is hoped that these functions may be partially shared between each spatial sub-channel, the formats were first investigated with DSP functions of resampling, normalization, dispersion compensation and polarization de-multiplexing first carried out independently on each core before combining for symbol detection and error counting of the 12-D formats. Fig. 6 shows a summary of the measured 12 dimensional modulation formats based on 16QAM (a, b) and 64QAM (c, d) in each polarization of 3 cores. Fig. 6 (a) shows the back-to-back measured plots of BER vs OSNR for the mean average uncoded 16QAM signals (24 bits/12-D symbol) and the 5 coded formats with k= 12, 11, 8, 7 and 4 with 24, 23, 20, 19 and 16 bits respectively in each 12-D symbol. For reference, simulated curves of the coded formats are also shown. Fig. 6(c) shows the equivalent plot for coded formats based on 64-QAM with each 3-core symbol coding 36, 35, 32, 31 and 28 bits for the same values of k. The received BER as a function of transmission distance with the same k values is shown in Fig. 6 (b) and Fig. 6 (d) for PDM-16QAM and PDM-64QAM formats respectively.

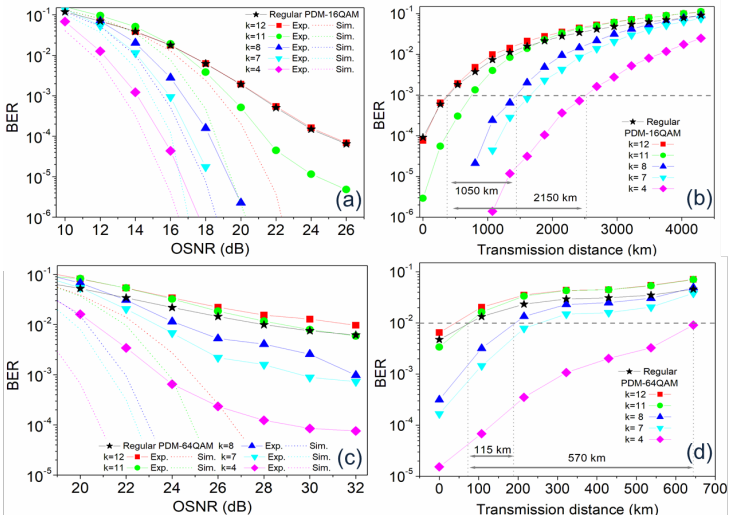

FIG. 6 - Comparison of 12D coded lattice formats over 3 MCF cores for k=4, 7, 8, 11 and 12 showing BER vs OSNR in back-to-back for (a) coded formats based on PDM-16QAM and (c) PDM-64QAM together with BER as a function of transmission distance for (b) formats based on PDM-16QAM and (d) PDM-64QAM.

Fig 6 (a) shows that the 12-D formats based on PDM-16QAM may be received with an implementation penalty of under 1 dB at a BER=1 $x10^{-2}$, similar to that observed for the regular PDM-16QAM. At the higher OSNR values of PDM-64QAM, large implementation penalties are observed for all formats. There is also evidence of error floors attributed to OSNR limitation and non-linearity of electrical amplifiers in both transmitter and receiver hardware that particularly affected the higher order formats. The k=12 coded formats both have the same spectral efficiency as the regular QAM formats and so represent an interesting point of comparison. In comparison to regular PDM-64QAM, there is a noticeable penalty in both OSNR and transmission distance for both the k=12 and k=11 format. This is believed to result from sub-optimal bit-mapping of the coded formats as well as additional implementation penalty for the 3 core formats arising from non-uniformity of hardware across the 3 transmitter, receiver and loop components.

Despite observed hardware limitations, for formats with k=8 or less, the coded modulation formats allow both a reduced required receiver OSNR, Fig 6. (a) and (c), and increased transmission reach, Figs. 6. (b) and (d), at the cost of spectral efficiency reduction. For a BER of 1 x 10^{-2}, and comparing the k=8 and k=4 formats based on 16QAM, we observe a reduction in OSNR requirement of 4.3 and 6.9 dB which translate to an increased transmission distance of 76% and 116% on the uncoded transmission distance of 1250 km at the same BER threshold. At lower BERs these formats show larger percentage reach gains. At a BER of 1 x 10^{-3} the 400km reach can be extended by 1050km (262%) and 2150 km (537%) by adopting the k=8 and k= 4 formats respectively.

For the coded 64QAM formats, it was not possible to compare at lower BERs due to hardware limitations, however at BER = 1 x 10^{-2} the 70 km transmission distance is increased by 115km (164%) for the k=8 format and 570km (814%) for the k=5 format. It is likely that the combination of the hardware limited reach of regular PDM-64QAM and the granularity of per span distance measurements, gives artificially high percentage gains of transmission distance. However, Fig. 6 (d) shows that the coded modulation formats can significantly improve reach for a relative modest loss of spectral efficiency of 11% and 22% respectively for the k=8 and k=4 formats. We note that it is likely that for systems targeting receiver BERs > 1 x 10^{-2} investing all coding overheard in soft-division FEC codes on regular QAM constellations may outperform coded modulation formats such as those presented in [42]. However, the results in Fig. 6 show that for application requiring lower receiver BERs or where latency requirements prohibit such FEC, these formats can offer improved performance and a flexible trade-off between throughput and transmission reach.

C. JOINT PHASE NOISE ESTIMATION

In addition to joint modulation, the set-up was also used to investigate the use joint digital-signal processing techniques for carrier-phase estimation (CPE). In optical transmission systems, CPE is typically performed on each fiber individually using blind methods such as Viterbi-Viterbi algorithm or blind phase search [43], [44]. However, as with other DSP functions, access to correlated spatial channels opens up the prospect of improved performance and processing efficiency. Previously, CPE of SSCs was first proposed for MCF transmission [16] and also demonstrated in multi-mode transmission [45]. More recently a pilot-aided multichannel phase-noise estimation algorithm was proposed [46] and investigated for MCF transmission [18]. In this section, we use experimental data generated using the set-up shown in Fig. 7 to investigate PDM-16QAM transmission with the 3 CPE strategies outlined as follows:

Separate processing – Phase-noise estimation is run independently on each spatial channel, and the resulting performance does not depend on the spatial correlation in the phase noise.

Master–slave processing – A single channel is selected for phase-noise estimation and the resulting estimates are used to compensate for all channels. This strategy allows for a lowered computational complexity in the receiver and is effective provided that the phase noise is identical in all channels. However, its performance can degrade quickly in the presence of inter-channel or inter-core phase drifts.

Joint processing – All channels are used in a cooperative manner to estimate the phase noise, as proposed in [46]. This strategy has the same performance as separate processing for uncorrelated phase noise, and in the case of correlated phase noise it will yield the best performance out of the considered strategies

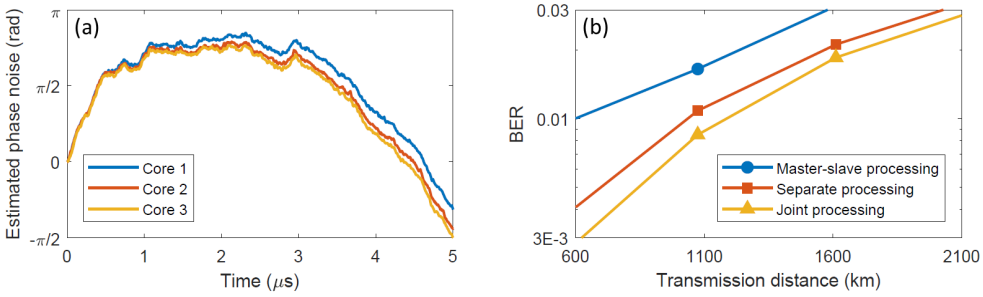

FIG 7. Comparison of different phase-noise estimation strategies in 3-core MCF PDM-16QAM transmission. (a) Estimated phase noise, averaged over the two polarizations in each core, showing a high degree of spatial correlation among the cores and (b) BER vs transmission distance.

Fig 7 (a) shows the correlation between the estimated phase noise over a single polarization of each spatial channel over a 5 μs period. The observed correlation explains why joint processing of spatial channels is able to increase the accuracy of the phase-noise estimation and ultimately improve the link quality with potential gains. The amount of phase noise and its spatial correlation ultimately determine what gains can be achieved, but the choice of modulation format and its interaction with the chosen CPE algorithm also has an impact. Moreover, the presence of inter-core phase drifts means that master–slave processing can be impaired in MCF systems. This is evident in Fig. 7 (b), which shows BER vs. transmission distance for the investigated CPE strategies with both separate and joint processing being carried out at 0.2% pilot overhead and master–slave processing at 1% pilot overhead. Master–slave processing appears to give the highest BERs at each distance due to the non-ideal phase-noise correlation. In contrast, joint processing gives an advantage over separate processing, increasing the transmission distance by approximately 200km at a BER of 1 x 10^{-2}. This result shows the potential of joint SDM channel processing to improve the overall performance in SDM systems, but also serves to highlight the lack of experimental studies on the impact of spatial channel skew on such experiments. We note that these results are obtained with good skew compensation of the MCF cores on each span and the impact of the path length accuracy was not investigated in detail. Whether similar gains can be observed with parallel SMF systems and if such gains can be applicable to long distance transmission and are compatible across networks with flexible path alignment remain open questions.

6. CONCLUSIONS

We have investigated the fiber and transmission characteristics of homogeneous, single-mode multi-core fibers (MCFs). Such MCFs are expected to be candidate fibers for early adoption of SDM fibers, due to their compatibility with existing single mode infrastructure. However, in addition to an improved spatial spectral efficiency the attractiveness of homogeneous MCFs hinges on whether the correlated propagation delay (skew) between cores enables benefits from joint processing and hardware sharing can exceed those in parallel single mode-fibers (SMFs). We first assessed the impact of inter-core crosstalk concluding that while some investigated homogeneous fibers are likely to impair long-distance transmission, it is possible to

design fibers with specific crosstalk characteristics to match the target environment. Next, we investigated skew in homogeneous MCFs, including a comparison with independent SMFs including over varying temperature showing significantly lower variations in propagation delay in homogeneous MCFs compared to SMFs. We then described MCF system experiments with independent modulation and parallel transmission and reception in 3 cores. We first showed flexible trade-off of reach and spectral efficiency in two families of 12-dimensional modulation formats based on 16-QAM and 64-QAM modulation. Finally, we showed gains in transmission distance can be achieved by adopting joint carrier phase estimation over individual core processing. While these results show the potential of homogeneous MCFs to out-perform parallel SMFs in addition to arguments of physical space, they further serve to highlight the need for more detailed investigation and quantification of system benefits.

REFERENCES

[1] D. J. Richardson, J. M. Fini, and L. E. Nelson, 'Space-division multiplexing in optical fibres', Nat. Photonics, vol. 7, no. 5, pp. 354–362, Apr. 2013.

[2] G. M. Saridis et al., 'Survey and Evaluation of Space Division Multiplexing: From Technologies to Optical Networks', IEEE Commun. Surv. Tutor., vol. 17, no. 4, pp. 2136–2156, 2015.

[3] T. Mizuno et al., 'Long-Haul Dense Space-Division Multiplexed Transmission Over Low-Crosstalk Heterogeneous 32-Core Transmission Line Using a Partial Recirculating Loop System', J. Light. Technol., vol. 35, no. 3, pp. 488–498, Feb. 2017.

[4] Roland Ryf et al. "High spectral efficiency mode-multiplexed transmission over graded-index multi-mode fiber" Proc. ECOC, paper Th3B.1, 2018

[5] J. Sakaguchi et al., 'Realizing a 36-core, 3-mode Fiber with 108 Spatial Channels', in Optical Fiber Communication Conference, 2015, pp. Th5C–2.

[6] K. Igarashi et al., '114 Space-Division-Multiplexed Transmission over 9.8-km Weakly-Coupled-6-Mode Uncoupled-19-Core Fibers', in Optical Fiber Communication Conference, 2015, pp. Th5C–4.

[7] D. Soma et al., '10.16-Peta-B/s Dense SDM/WDM Transmission Over 6-Mode 19-Core Fiber Across the C+L Band', J. Light. Technol., vol. 36, no. 6, pp. 1362–1368, Mar. 2018.

[8] B. J. Puttnam et al., '2.15 Pb/s transmission using a 22 core homogeneous single-mode multi-core fiber and wideband optical comb', in Optical Communication (ECOC), 2015 European Conference on, 2015, pp. 1–3.

[9] A. Turukhin et al., '105.1 Tb/s power-efficient transmission over 14,350 km using a 12-core fiber', in 2016 Optical Fiber Communications Conference and Exhibition (OFC), 2016, pp. 1–3.

[10] T. Mizuno et al., 'Dense Space Division Multiplexed Transmission Over Multicore and Multimode Fiber for Long-haul Transport Systems', J. Light. Technol., vol. 34, no. 6, pp. 1484–1493, Mar. 2016.

[11] A. Turukhin et al., 'Demonstration of 0.52 Pb/s Potential Transmission Capacity over 8,830 km using Multicore Fiber', in ECOC 2016; 42nd European Conference on Optical Communication, 2016, pp. 1–3.

[12] I. Morita, K. Igarashi, H. Takahashi, T. Tsuritani, and M. Suzuki, 'Trans-oceanic class ultra-long-haul transmission using multi-core fiber', Opt. Express, vol. 22, no. 26, p. 31761, Dec. 2014.

[13] Y. Lee et al., 'Multi-core fiber technology for optical-access and short-range links', in 2014 12th International Conference on Optical Internet 2014 (COIN), 2014, pp. 1–2.

[14] K. Tanaka et al., 'Automatic Impairment-Aware Optical Path Switching in Multicore Fiber Link Based on Multiring Structure', J. Light. Technol., vol. 33, no. 14, pp. 3060–3068, Jul. 2015.

[15] N. Amaya et al., 'Fully-elastic multi-granular network with space/frequency/time switching using multi-core fibres and programmable optical nodes', Opt. Express, vol. 21, no. 7, p. 8865, Apr. 2013.

[16] M. D. Feuer et al., 'Joint Digital Signal Processing Receivers for Spatial Superchannels', IEEE Photonics Technol. Lett., vol. 24, no. 21, pp. 1957–1960, Nov. 2012.

[17] B. J. Puttnam et al., 'Modulation formats for multi-core fiber transmission', Opt. Express, vol. 22, no. 26, p. 32457, Dec. 2014.

[18] M. Grassl, '"Code tables: Bounds on the parameters of various types of codes, online, codetables.de'. .

[19] R. Ryf et al., 'Long-Haul Transmission over Multi-Core Fibers with Coupled Cores', in 2017 European Conference on Optical Communication (ECOC), 2017, pp. 1–3.

[20] N. K. Fontaine et al., 'Coupled-Core Optical Amplifier', in Optical Fiber Communication Conference Postdeadline Papers (2017), paper Th5D.3, 2017, p. Th5D.3.

[21] J. C. Alvarado-Zacarias et al., 'Coupled-Core EDFA Compatible with FMF Transmission', in Optical Fiber Communication Conference Postdeadline Papers (2018), paper Th4A.3, 2018, p. Th4A.3.

[22] B. J. Puttnam et al., 'Inter-Core Skew Measurements in Temperature Controlled Multi-Core Fiber', in 2018 Optical Fiber Communications Conference and Exposition (OFC), 2018, pp. 1–3.

[23] R. S. Luis et al.,, 'On the Use of High-Order MIMO for Long-Distance Homogeneous Single-Mode Multicore Fiber Transmission', in 2017 European Conference on Optical Communication (ECOC), 2017, pp. 1–3.

[24] T. Hayashi et al., 'Design and fabrication of ultra-low crosstalk and low-loss multi-core fiber', Opt. Express, vol. 19, no. 17, pp. 16576–16592, 2011.

[25] R. S. Luís et al., ‘Time and Modulation Frequency Dependence of Crosstalk in Homogeneous Multi-Core Fibers’, J. Light. Technol., vol. 34, no. 2, pp. 441–447, Jan. 2016.
[26] J. M. Fini et al.,, ‘Statistical Models of Multicore Fiber Crosstalk Including Time Delays’, J. Light. Technol., vol. 30, no. 12, pp. 2003–2010, Jun. 2012.
[27] A. V. T. Cartaxo et al.,, ‘Dispersion Impact on the Crosstalk Amplitude Response of Homogeneous Multi-Core Fibers’, IEEE Photonics Technol. Lett., vol. 28, no. 17, pp. 1858–1861, Sep. 2016.
[28] G. Rademacher et al., ‘Crosstalk dynamics in multi-core fibers’, Opt. Express, vol. 25, no. 10, pp. 12020–12028, May 2017.
[29] B. J. Puttnam et al., ‘Inter-Core Crosstalk Spectrum and Penalty Measurements in 7-Core Fiber’, in 2017 European Conference on Optical Communication (ECOC), 2017, pp. 1–3.
[30] B. J. Puttnam et al., ‘High Capacity Transmission Systems Using Homogeneous Multi-Core Fibers’, J. Light. Technol., vol. 35, no. 6, pp. 1157–1167, Mar. 2017.
[31] A. Sano et al., ‘409-Tb/s + 409-Tb/s crosstalk suppressed bidirectional MCF transmission over 450 km using propagation-direction interleaving’, Opt. Express, vol. 21, no. 14, p. 16777, Jul. 2013.
[32] K. Takenaga et al., ‘Reduction of crosstalk by trench-assisted multi-core fiber’, in Optical Fiber Communication Conference, 2011, p. OWJ4.
[33] Y. Sasaki et al., ‘Trench-assisted low-crosstalk few-mode multicore fiber’, in Optical Communication (ECOC 2013), 39th European Conference and Exhibition on, 2013, p. Mo.3.A.5.
[34] Y. Amma et al., ‘High-density multicore fiber with heterogeneous core arrangement’, in 2015 Optical Fiber Communications Conference and Exhibition (OFC), 2015, pp. 1–3.
[35] T. Hayashi et al., ‘Characterization of interconnect multi-core fiber cable: Mechanical/thermal characteristics and inter-core crosstalk of the straightened cable’, 2016, pp. 92–93.
[36] R. S. Luis et al., ‘Impact of spatial channel skew on the performance of spatial-division multiplexed self-homodyne transmission systems’, in Photonics in Switching (PS), 2015 International Conference on, 2015, pp. 37–39.
[37] M. Koshiba, K. Saitoh, and Y. Kokubun, ‘Heterogeneous multi-core fibers: proposal and design principle’, IEICE Electron. Express, vol. 6, no. 2, pp. 98–103, 2009.
[38] G. Saridis et al., ‘Dynamic Skew Measurements in 7, 19 and 22-core Multi Core Fibers’, presented at the OECC/PS 2016, 2016.
[39] R. S. Luís et al.,, ‘Comparing inter-core skew fluctuations in multi-core and single-core fibers’, in 2015 Conference on Lasers and Electro-Optics (CLEO), 2015, p. SM2L.5.
[40] T. A. Eriksson et al., ‘K-Over-L Multidimensional Position Modulation’, J. Light. Technol., vol. 32, no. 12, pp. 2254–2262, 2014.
[41] G. Rademacher et al., ‘Experimental investigation of a 16-dimensional modulation format for long-haul multi-core fiber transmission’, in 2015 European Conference on Optical Communication (ECOC), 2015, pp. 1–3.
[42] E. Agrell et al., ‘Modulation and Detection for Multicore Superchannels with Correlated Phase Noise’, in Conference on Lasers and Electro-Optics (2018), paper SM4C.3, 2018, p. SM4C.3.
[43] A. Viterbi, ‘Nonlinear estimation of PSK-modulated carrier phase with application to burst digital transmission’, IEEE Trans. Inf. Theory, vol. 29, no. 4, pp. 543–551, Jul. 1983.
[44] T. Pfau, S. Hoffmann, and R. Noe, ‘Hardware-Efficient Coherent Digital Receiver Concept With Feedforward Carrier Recovery for M -QAM Constellations’, J. Light. Technol., vol. 27, no. 8, pp. 989–999, Apr. 2009.
[45] R. G. H. van Uden et al., ‘Single DPLL Joint Carrier Phase Compensation for Few-Mode Fiber Transmission’, IEEE Photonics Technol. Lett., vol. 25, no. 14, pp. 1381–1384, Jul. 2013.
[46] A. Alfredsson, E. Agrell, and H. Wymeersch, ‘Iterative Decoding and Phase-Noise Compensation for Multichannel Optical Transmission’, ArXiv180402263 Cs Math, Apr. 2018.